J Therm Anal Calorim (2012) 109:1019–1032
DOI 10.1007/s10973-011-1940-8

Functionalisation of polypropylene non-woven fabrics (NWFs)

Functionalisation by oxyfluorination as a first step for graft polymerisation

Viktória Vargha · Avashnee Chetty · Zsolt Sulyok · Judith Mihály · Zsófia Keresztes · András Tóth · István Sajó · László Korecz · Rajesh Anandjiwala · Lydia Boguslavsky

Received: 26 April 2011 / Accepted: 20 September 2011 / Published online: 21 October 2011

Abstract Surface oxyfluorination had been carried out on polypropylene non-woven fabric (PP NWF) samples of different morphologies and pore sizes. The modified surfaces were characterised by Attenuated Total Reflectance Fourier Transform InfraRed (ATR-FTIR)-spectroscopy, FTIR imaging microscopy, X-Ray Photoelectron Spectroscopy (XPS), Electron Spin Resonance (ESR) spectroscopy, Differential Scanning Calorimetry (DSC), X-Ray Diffraction (XRD) analysis, Scanning Electron Microscopy (SEM), dynamic rheometry and Thermo-Gravimetry (TG). ATR-FTIR and XPS techniques revealed the presence of –CF, $–CF_2$, –CHF and –C(O)F groups. The formed –C(O)F groups mostly got hydrolysed to –COOH groups. The C=O groups of alpha-haloester, and the C=C stretching of the formed –CF=C(OH)– groups could also be detected. Long-lived radicals could be detected on the functionalised surfaces as middle-chain peroxy radicals by ESR spectroscopy. SEM micrographs showed slight roughening of the oxyfluorinated surfaces. Oxyfluorination had no significant effect on the crystalline structure and phase composition of the PP NWF samples supported by DSC and XRD measurements. The molecular mass of the samples were unaffected by the oxyfluorination treatment as proved by oscillating rheometry. The surface modification, however, significantly affected the thermal decomposition but not affected the thermo-oxidative decomposition of PP NWFs. Different morphologies and pore sizes of PP NWF samples resulted in reproducibility of the findings, although did not substantially affect surface functionalisation.

Keywords Oxyfluorination · PP non-woven fabrics · ATR-FTIR · FTIR-imaging · XPS · ESR · SEM · DSC · WAXS · Dynamic rheometry · TG

V. Vargha (✉) · Z. Sulyok
Budapest University of Technology and Economics, Department of Physical Chemistry and Material Science, Műegyetem rkp. 3. H/1, Budapest 1111, Hungary
e-mail: vvargha@mail.bme.hu

A. Chetty
CSIR Materials Science and Manufacturing, Polymers and Composites, P. O. Box 395, Pretoria 0001, South Africa

J. Mihály · Z. Keresztes · I. Sajó
Chemical Research Center of the Hungarian Academy of Sciences, Institute of Nanochemistry and Catalysis, Pusztaszeri út 59-67, Budapest 1025, Hungary

A. Tóth
Chemical Research Center of the Hungarian Academy of Sciences, Institute of Materials and Environmental Chemistry, Pusztaszeri út 59-67, Budapest 1025, Hungary

L. Korecz
Chemical Research Center of the Hungarian Academy of Sciences, Institute of Structural Chemistry, Pusztaszeri út 59-67, Budapest 1025, Hungary

R. Anandjiwala · L. Boguslavsky
CSIR Materials Science and Manufacturing, Polymers & Composites Competence Area, POBox 1124, Summerstrand, Port Elizabeth 6000, South Africa

Introduction

Commodity polyolefins, namely, polyethylene and polypropylene (PP) are widely used in industry because of their low cost, ease of processing, good mechanical properties, and excellent chemical resistance. These polymers, however, have low surface tension, poor adhesion and insufficient chemical functionality which limit their use in certain

applications. There are a number of pre-treatment techniques commonly used to activate polymer surfaces, such as plasma modification, gamma-irradiation, UV-irradiation, ozonation, surface-graft polymerisation, chemical reaction and flame treatment.

In recent years, surface fluorination has proved to be an effective pre-treatment technique for increasing the wettability, adhesion and barrier properties of hydrocarbon polymers [1–5]. Fluorination is attractive over other functionalising methods since it is less invasive, e.g. compared to radiation, is a dry technology, can be used to modify articles of any shape, and can be conducted at relatively low temperatures in a low vacuum. In addition, fluorine gas is highly reactive and can penetrate polymer surfaces to large depths up to about 10 μm, while the bulk properties mainly remain unchanged [6].

During surface fluorination, hydrocarbon polymer materials are exposed to diluted fluorine gas mixture, which reacts with the polymer surface via a free-radical chain reaction mechanism (see Eqs. 1 and 2), resulting in the formation of a very thin, partially fluorinated polymer surface layer [2].

$$R - H + F_2 \rightarrow R^* + HF + F^* \quad (1)$$

$$R^* + F_2 \rightarrow R - F + F^* \quad (2)$$

The thickness of the fluorinated layer is dependent on fluorine gas diffusion through the sample [7], which is controlled by the reaction variables, such as polymer type and structure, fluorine partial pressure, fluorine concentration, reaction time and reaction temperature. The importance of diluting fluorine gas with an oxygen-free inert gas (such as nitrogen and helium) to prevent fragmentation of the carbon backbone has been reported in the literature [7–9]. It is however, still believed by many research groups that oxidation always accompanies fluorination, since commercial fluorine is known to contain oxygen as an impurity [10, 11].

During oxyfluorination, hydrocarbon polymers are simultaneously fluorinated and functionalised by significant amounts of oxygen (see Eq. 3) in either in the fluorinating reaction mixture or by the use of oxygen directly as a reactive diluting gas [8].

$$R^* + O_2 \rightarrow R - O - O^* \quad (3)$$

The existences of acid fluoride groups and peroxides as well as crosslinking of the surface during oxyfluorination have been reported [7, 12]. The ratio of the fluorocarbon radicals to hydrocarbon radicals is higher during fluorination than in oxyfluorination, with the former having been preferred because of its longer life-time. The rate of the fluorination reaction in the presence of oxygen is much slower than that of a fluorination reaction in which nitrogen is used as the diluting gas. This is to be expected since oxygen, which is very reactive towards radicals, inhibits the reaction by reacting with the radicals that are formed during fluorination (Eq. 3) to form peroxy radicals which are much less reactive than is the R^* radical. Jeong et al. utilised the peroxy radicals generated by oxyfluorination to assist in graft polymerisation for modifying the surfaces of low-density polyethylene (LDPE) films [13].

The possibility of etching the PP surface during oxyfluorination has also been suggested [2]. The effects of oxygen/fluorine gas mixtures on a PP surface include improved wettability, a significant increase in polarity and a roughening of the surface resulting from the exothermic nature of the reaction [2, 14]. Sanderson et al. have found that PP had a higher fluorination rate than polyethylene [7, 14].

Direct fluorination may also result in the formation of peroxy radicals because of the presence of some per cent oxygen in nitrogen as diluting gas and the trace of oxygen in commercial fluorine gas. There remains uncertainty, however, about the mechanism by which oxygen is introduced into the surfaces of fluorinated polymers and about the nature of the functionalisation. Kharitonow and co-workers [15–18] have confirmed the formation and termination of long-lived peroxy radicals and short-lived radicals by the 'direct fluorination' of various polymers. However, according to Sanderson and co-workers, no indication of oxygen-containing functionalities was obtained for PP samples fluorinated by 10:90 F_2:N_2 gas mixture, and even after long fluorination times, functionalisation was limited to the formation of only –CHF and CF_2 groups [3].

In this study, oxyfluorination of NWFs based on PP have been investigated as a pre-treatment step to impregnate reactive functional groups on the surface of the PP for post-graft polymerisation. The aim of this study is to modify the surface of five PP open-porous NWFs with different mean flow pores and densities by an oxyfluorination pre-treatment method. We are reporting on five samples to see the reproducibility of the oxyfluorination treatment, as well as to see the effect of pore size and NWF density on the extent of fluorination, since the more porous structure should enable better diffusion and penetration of the gas into the scaffold. The chemical and physical characterisations of the oxyfluorinated NWFs compared to virgin PP are the subject of this article. Characterisation techniques include attenuated total reflectance fourier transform infrared (ATR-FTIR)-spectroscopy, FTIR imaging microscopy, X-ray photoelectron spectroscopy (XPS), electron spin resonance (ESR) spectroscopy, differential scanning calorimetry (DSC), X-ray diffraction (XRD) analysis, scanning electron microscopy (SEM), dynamic rheometry and thermo-gravimetry (TG). The oxyfluroinated NWFs

Table 1 PP non-woven fabrics (NWFs) used for the experiments

NWF	Preparation	Depth of penetration/mm /mm	Fibre linear density /dtex	Area density /gm^{-2}
pPP-1	Needle-punched	6	6.7	125
pPP-2	Needle-punched	10	2.2	150
pPP-3	Needle-punched	10	6.7	200
pPP-4	Needle-punched + calendered	n.a.	2.2	n.a.
pPP-5	Needle-punched	10	6.7	260

NWF pPP refers to pure (virgin or untreated) polypropylene

Table 2 Pore size of PP non-woven fabrics (NWFs) used for the experiments determined by PMI Capillary Flow Porometer according to Test method 6212005-134 corresponding to ASTM E 1294

NWF	Minimum/μm	MFP[a]/μm	Maximum/μm
pPP-1	7	97	384
pPP-2	5	46	71
pPP-3	7	144	312
pPP-4	7	85	185
pPP-5	6	108	208

[a] The mean flow pore (MFP) diameter is such that fifty percent of flow is through pores larger than MFP diameter and the rest of the flow is through smaller pores. The mean flow pore diameter is a measure of permeability

prepared in this study have been used in a subsequent study for the graft.

Experimental

Materials

PP non-woven fabrics (NWFs) have been prepared in-house at the CSIR Materials Science and Manufacturing in Port Elizabeth by a needle-punching technology [19]. The characteristics of the non-woven samples are summarised in Tables 1 and 2.

Oxyfluorination

The PP NWFs were oxyfluorinated at Pelchem Pty Ltd. (South Africa) by a proprietary method whereby the NWFs are loaded into a reaction vessel (RV). The RV is purged and partially evacuated, and then a 20/80 vol/vol F_2:N_2 gas mixture is introduced for a certain time-period. The gas mixture is then cycle purged from the RV to complete the fluorination process. Owing to the partial vacuum, and the presence of some air in the reactor, and with the 4–5 vol/% oxygen impurity present in nitrogen, the process can be referred to as oxyfluorination.

Methods of characterisation

Attenuated total reflectance infrared (ATR-FTIR) spectroscopy

Infrared spectra were collected by a Varian Scimitar 2000 FTIR spectrometer using MCT (mercury–cadmium–tellur) detector equipped with a single reflection ATR unit (SPECAC 'Golden Gate') with diamond ATR element (active surface: 0.6 × 0.6 mm^2). All spectra were recorded by co-addition of 128 individual spectra with 4 cm^{-1} resolution.

FTIR imaging

Homogeneity/inhomogeneity had been studied by creating chemical images of selected surface groups/species. FTIR images were collected on individual oxyfluorinated fibres by means of a Varian FTS-7000 spectrometer coupled to a microscope configuration (UMA-600) with an FPA (Focal Plane Array) multidetector (Stingray) system consisting of a 64 × 64 MCT detector units. For the measurements, the reflexion technique was selected, using 8 cm^{-1} resolution and 16 scans. To each detector unit (pixel) corresponds on average, ~5.5 μm lateral resolution.

X-ray photoelectron spectroscopy (XPS)

XPS spectra were taken by a Kratos XSAM800 spectrometer, using Mg Kα radiation, 225 W X-ray power, and fixed analyser transmission (FAT) mode. The survey and detailed spectra were recorded with 80 and 40 eV pass energies, respectively. The survey spectra were taken in the kinetic energy range of 100–1,300 eV with a resolution of 0.5 eV, while the resolution of the detailed spectra of the selected ranges was 0.1 eV. Four sweeps were applied to improve the signal-to-background ratio. The spectra were referenced to the C1s line (binding energy, BE = 285 eV). Data acquisition and processing were performed by the Kratos Vision 2 program.

Electron spin resonance (ESR) spectroscopy

ESR spectra were obtained on a Bruker Elexsys 500 spectrometer operating at X-band frequencies (~9–10 GHz). Spectra were recorded as first derivatives of microwave absorption of a total 10–20 scans, at ambient temperature, using 2 mW microwave power, modulation frequency = 100 kHz, modulation amplitude = 1 G.

Scanning electron microscopy (SEM)

Surface morphology was monitored with a JEOL JSM 6380 LA scanning electron microscope. The samples were coated with gold to make imaging possible. For attaining the best image quality, the acceleration voltage was varied between 5 and 15 kV. The detection modes are indicated in the bottom-right corner of each image.

Differential scanning calorimetry (DSC)

For DSC measurements a Perkin Elmer DSC 7 was used. About 5 mg of the sample was heated from −60 to +250 °C with a heating rate of 10 °C min^{-1} followed by a cooling step and a second heating both with the same cooling and heating rate. Stream of purging nitrogen gas was 40 mL min^{-1}. The course of measurements is represented by Fig. 1.

Wide-angle X-ray scattering (WAXS)

WAXS scans were obtained in a Philips model PW 3710 based PW 1050 Bragg–Brentano parafocusing goniometer using CuKα radiation ($\lambda = 0.15418$ nm), graphite monochromator and proportional counter.

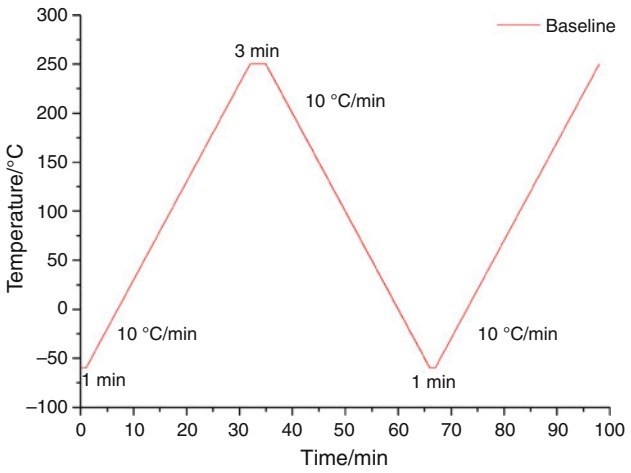

Fig. 1 Program of DSC measurements

Dynamic rheometry

For rheological measurements an Anton Paar MCR 301 dynamic rheometer was used. Change in complex viscosity with frequency was tested in the frequency range of 600–0.1 s^{-1} with a plate–plate arrangement and a slit distance of 1 mm at 180 ± 0.2 °C. The calculated shear rate interval is 29.2–0.005 s^{-1}.

Thermogravimetric analysis (TG)

Thermal behaviour and decomposition of PP and oxyfluorinated PP NWFs were tested with a Perkin Elmer TG 6. Approx. 10 mg sample was heated from 30 to 700 °C in purging nitrogen gas with a temperature rate of 10 °C/min. Thermo-oxidative degradation was tested in purging oxygen.

Results and discussion

Chemical composition of the surface of NWFs detected by ATR-FTIR spectroscopy and FTIR imaging

The results of ATR-FTIR spectroscopy for untreated and oxyfluorinated PP non-wovens (pPP4 and oPP4) are represented in Fig. 2.

Fluorination resulted in the appearance of the absorption bands of newly formed groups compared to untreated PP. The broad band in the range of 1,000–1,300 cm^{-1} can be assigned to –CF and $–CF_2$ groups. The bands maxima at about 1,191 and 1,079 cm^{-1} correspond to the symmetric stretching vibrations of the $–CF_2$ group and the C–F stretching vibration in –CF, –CHF, and –C(O)F groups, respectively [20, 21]. The absorption bands in the range of 1,900–1,600 cm^{-1} refer to the formed C=O groups after oxyfluorination. The most intensive absorption at 1,727 cm^{-1} can be assigned to the C=O stretching vibration of the formed –COOH groups. The formation of the latter may be the result of hydrolysis of the –COF groups on the effect of moisture. As a result of hydrolysis a broad absorption band can be detected in the fluorinated samples in the vicinity of 3,346 cm^{-1} characteristic to the associated –OH groups. The weak band at 1,850 cm^{-1} can be attributed to carbonyl vibration in the unhydrolysed –C(O)F groups. At 1,780 cm^{-1} the C=O stretching vibration of alpha-haloester, at 1,627 cm^{-1} the C=C stretching of the formed –CF=C(OH)– groups could be detected [22]. Owing to the penetration depth of the ATR-FTIR method (around 10 μm), reacted products included into the oxyfluorinated layer are also observed.

The integrated area under the C=O absorption bands of COOH groups, as well as of F-containing groups are

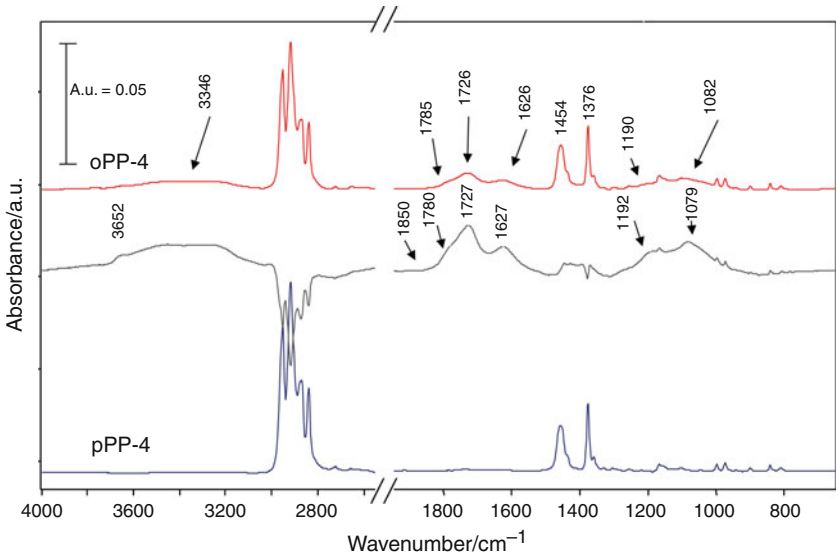

Fig. 2 ATR-FTIR spectra of NWF before (pPP-4) and after oxyfluorination (oPP-4). Difference spectrum is shown in the middle

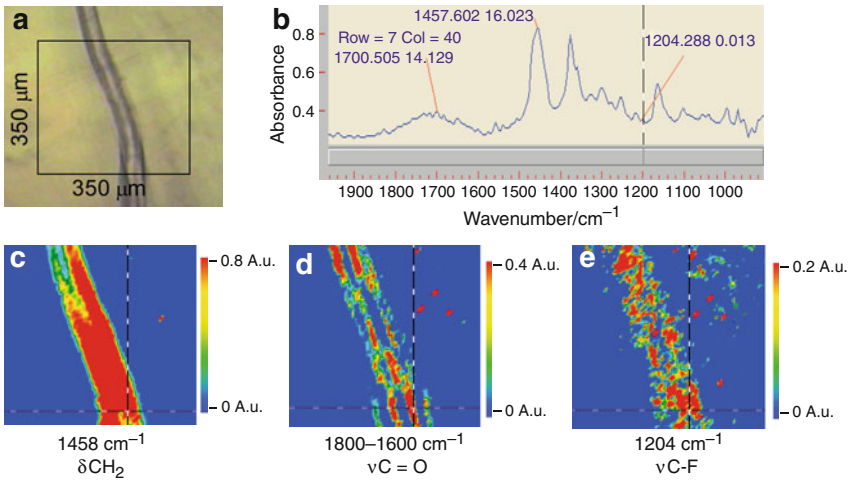

Fig. 3 Optical (**a**) and chemical (**c**, **d**, **e**) images of the oxyfluorinated samples focusing on a single fibre (oPP-4). The chemical images are constructed from areas under selected band intensities reflecting surface distribution of characteristic surface species. **b** is a characteristic spectrum detected by a selected detector element (pixel) corresponding to a sample area around $5.5 \times 5.5\ \mu m^2$ collected in reflection mode

relatively higher in oPP-4 than in oPP-5. This is supported also by XPS measurements.

The IR images of the oxyfluorinated samples are shown in Fig. 3.

Taking into consideration the geometry of the fibre sample, we can assume that the fluorine-containing species are distributed rather inhomogeneously penetrating deeply into the fibre interior, and the oxygen-containing species resulted as a consequence of hydrolysis are on the fibre surface.

Table 3 Surface composition of the oxyfluorinated NWF samples as revealed by XPS

Sample	F/at%	F/mass%	O/at%	O/mass%	C/at%	C/mass%
oPP-1	21.5	28.3	22.7	25.1	55.8	46.5
oPP-2	26.7	34.6	20.6	22.4	52.7	43.1
oPP-3	30.7	38.9	20.6	22.0	48.7	39.1
oPP-4	27.4	35.0	23.2	25.0	49.4	40.0
oPP-5	26.5	34.4	19.9	21.7	53.6	44.0

Surface analysis by XPS

The surface compositions obtained by XPS for the five oxyfluorinated samples are summarised in Table 3.

Pore size did not have any effect on the degree of functionalisation. Since fluorination is a gas surface treatment, it is assumed that a more porous NWFs will enable better diffusion of the gas into the structure. As a result of oxyfluorination, significant amounts of fluorine and oxygen could be detected on the surface of the samples. The concentration of fluorine atoms was found to be in the range of 21.5–31 at% (28–39 mass%) and that of oxygen atoms between 20 and 23 at% (22–25 mass/%). Figure 4 shows typical F 1s, O 1s and C 1s spectra for the oxyfluorinated PP

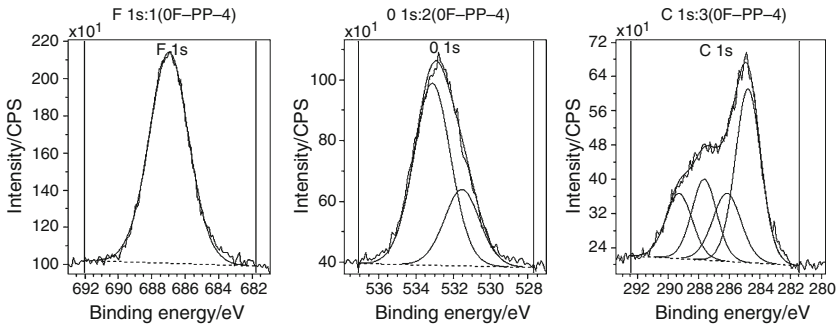

Fig. 4 Typical F 1s, O 1s, and C 1s peaks of oxyfluorinated non-woven PP fibres

samples. The F 1s peak is symmetric, centred at 687.0 eV, testifying to the presence of C–F bonds [23]. The O 1s peak is asymmetric, suggesting the presence of O in bonding modes like C–O at 533.2 eV and C=O at 531.6 eV [23].

The C 1s peak can be resolved into several components. Neglecting the minor secondary shifts, the following assignments can be made: C–C and C–H at 285 eV, C–O at 296.4 eV, C=O, O–C–O, and C–F states at 287.9 eV and O=C–O at about 289.4 eV [23].

In case of direct static fluorination hydrogen atoms are substituted by fluorine, double and conjugated bonds are saturated with fluorine. Crosslinking (formation of C–C bonds) and destruction of C–C bonds may also occur. In oxyfluorination, i.e. treatment of polymeric materials with fluorine–oxygen mixtures, C=O, COF, O=C–O and COOH groups can be inserted onto the polymer chains [15].

Both ATR-FTIR spectroscopy and XPS analysis support the presence of oxygen-containing groups on the surface of our functionalised NWF samples. Despite the applied process of fluorination, meaning that a mixture of 20/80 vol/vol fluorine/nitrogen gas was used, the surface of our treated samples is abundant with oxygen-containing groups. Oxygen was present during the fluorination process since the reactor was only partially evacuated. In addition, some oxygen may have been entrapped in the loose structure of NWFs, on the surface of the fluorinating vessel, and it may also have been present as an impurity (cca 4–5 vol/%) in the nitrogen gas. Another noteworthy observation is the fact, that –C(O)F groups could still be detected on all our treated surfaces. These groups should have hydrolysed on long time exposure to atmospheric conditions. Sanderson et.al. investigated the kinetics of hydrolysis of the –C(O)F groups. They have found that the hydrolysis of oxyfluorinated PP was initially fast, but levelled off after about 4 h. After 40 h of exposure to atmospheric conditions, some unhydrolysed groups still remained. In comparison with other surface modification techniques, fluorine atoms penetrate the surface of PP to

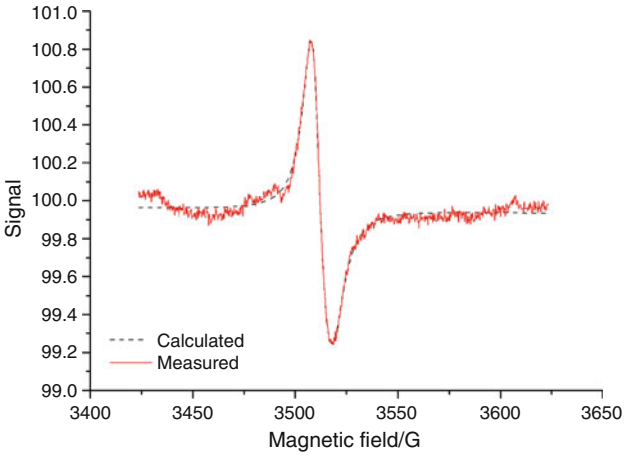

Fig. 5 Experimental and simulated ESR spectra of oxyfluorinated sample 2 (oPP-2)

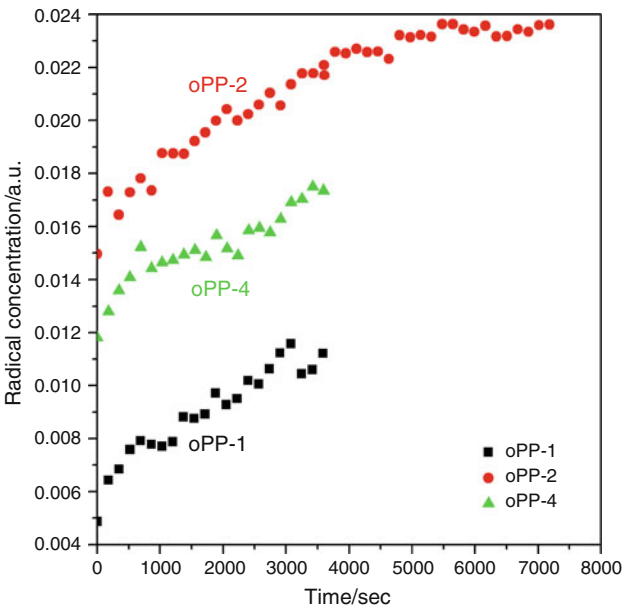

Fig. 6 The change in radical concentration with time at 70 °C (the temperature of grafting)

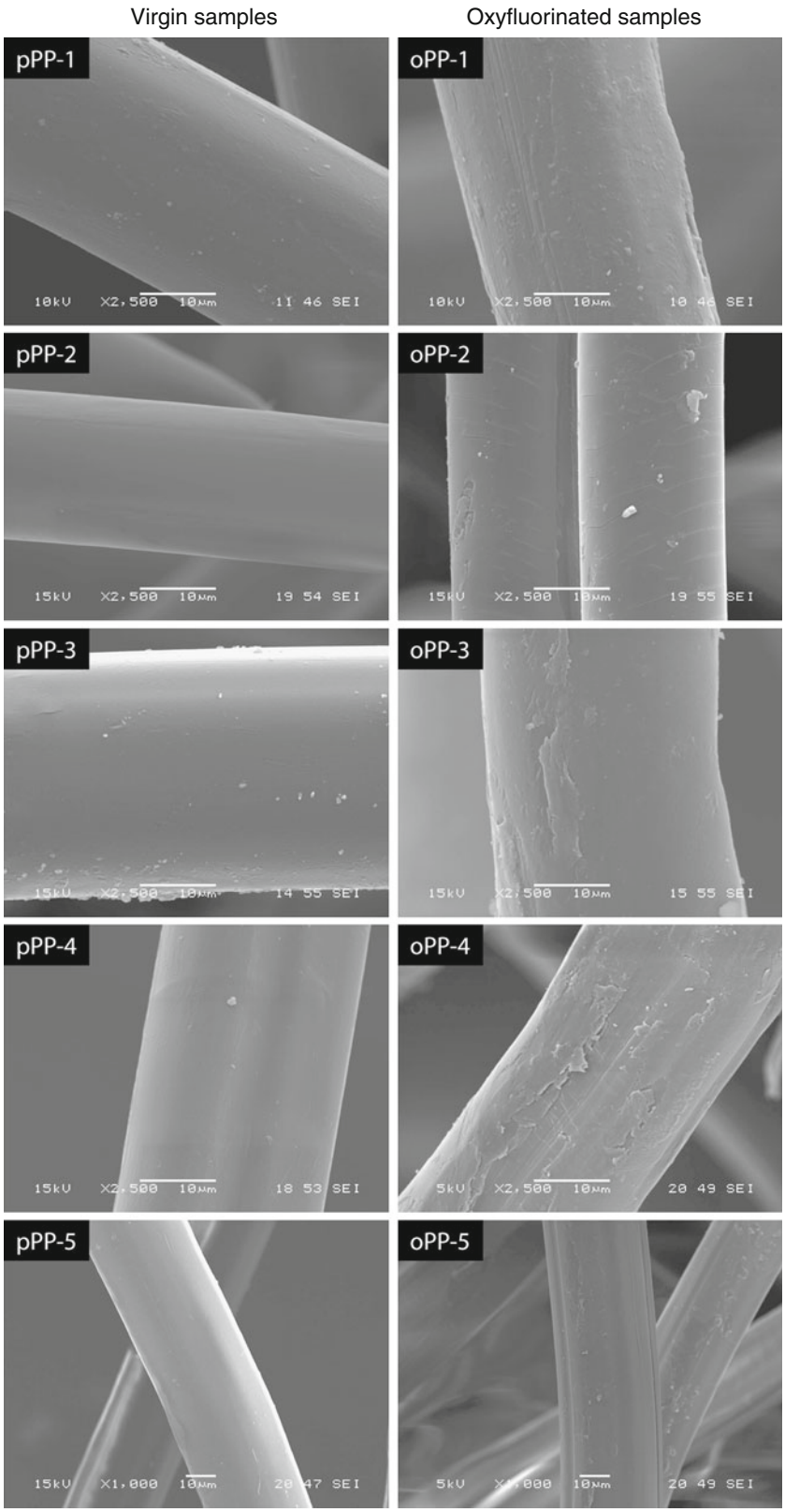

Fig. 7 SEM micrographs of virgin and oxyfluorinated PP NWFs

relatively great depths, the extent of which depends upon treatment conditions. The plateau in the hydrolysis curve may indicate the inability of atmospheric moisture to reach the unreacted groups deep in the polymer sample, especially since the barrier properties of the fluorinated and oxyfluorinated layers are well known [3].

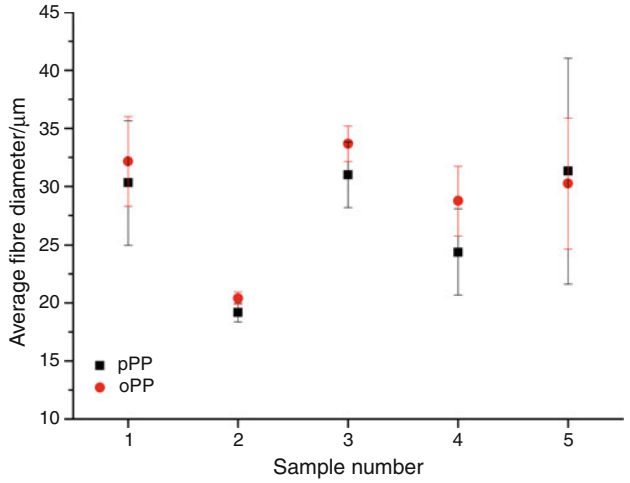

Fig. 8 The average diameter of the fibres of pPP and oPP NWF samples

Table 4 Glass transition temperatures of virgin and oxyfluorinated NWF samples

Sample	T_g First heating	T_g Cooling	T_g Second heating
pPP-1	n.d.	3.8	−2.1
oPP-1	0.5	n.d.	n.d.
pPP-2	5.9	−5.0	5.4
oPP-2	n.d.	−4.7	n.d.
pPP-3	n.d.	n.d.	n.d.
oPP-3	n.d.	−3.5	n.d.
pPP-4	3.08	−4.7	−3.7
oPP-4	n.d.	5.3	n.d.
pPP-5	n.d.	−5.8	n.d.
oPP-5	n.d.	0.1	n.d.

n.d. not detectable

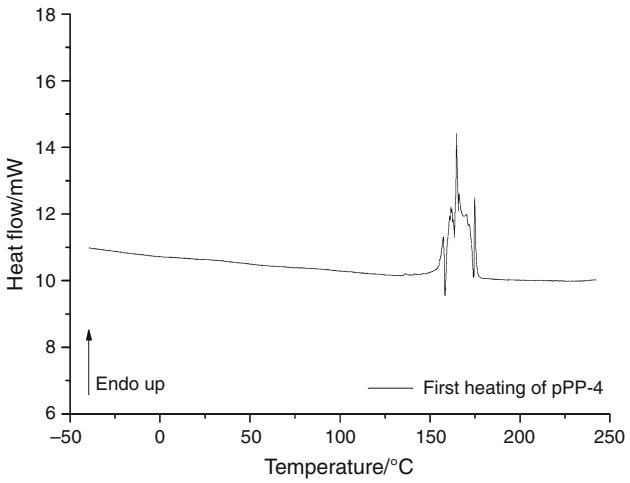

Fig. 9 The splitting of the enthalpy peak of pPP-4 during the first DSC heating step

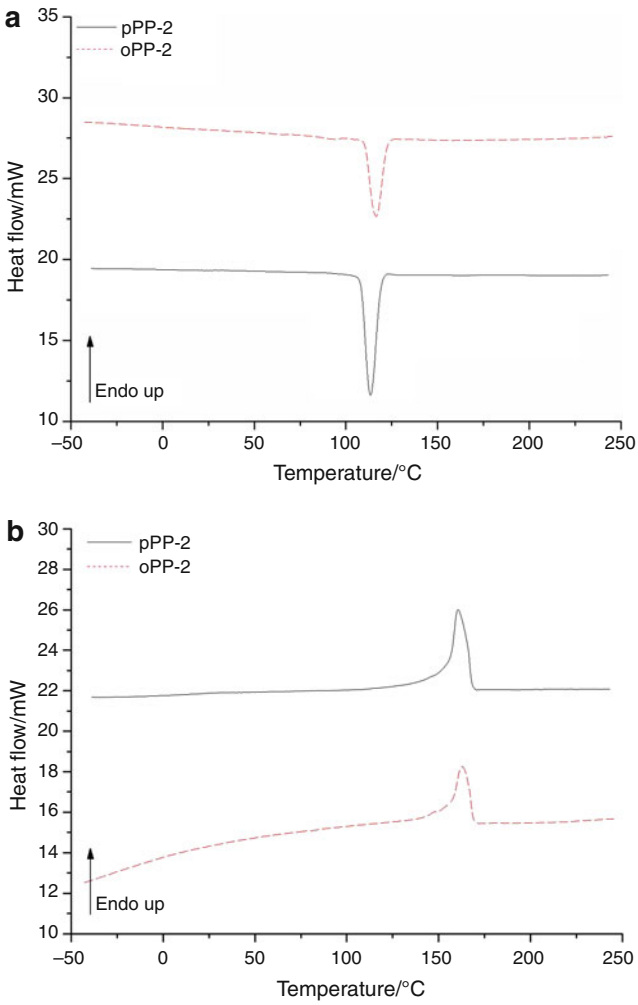

Fig. 10 Results of DSC analysis of virgin and oxyfluorinated NWF sample 2 (**a** 1st cooling, **b** 2nd heating)

Detection of long-lived radicals on the surface of oxyfluorinated NWF by ESR-spectroscopy

Weak asymmetric singlet absorption signals were observed for all of the oxyfluorinated NWFs, indicating the presence of long-lived free radicals in the polymer structure. The structureless asymmetric line shape can be interpreted in several different ways. The best fit was obtained in case of simple g anisotropy $g_{\perp}$=2.0022, $g_{\|} = 2.0054$. These values correspond to midchain peroxy radical [24]. Experimental and simulated spectra of oxyfluorinated sample 2 (oPP-2) is represented by Fig. 5.

In polymers treated with fluorine–oxygen mixtures, a controlled amount of long-lived peroxy radicals are generated [16]. Peroxy radicals terminate faster than fluoro-radicals [17]. The radicals formed in fluorinated polymers are long-lived ones; their amount is decreased by a factor of 2 in several hours at room temperature—from 1 to 15 h depending on the polymer nature [16].

Table 5 Data of crystallisation of PP-NWFs from 1st DSC cooling

Sample	T_{onset}/°C	T_p/°C	T_{end}/°C	ΔH/mWg^{-1}
pPP-1	117.6	113.0	109.1	−99.1
oPP-1	125.3	119.0	113.4	−93.4
pPP-2	119.0	113.3	108.3	−98.2
oPP-2	122.3	116.5	110.4	−99.1
pPP-3	118.1	113.5	109.3	−92.4
oPP-3	126.4	119.5	113.9	−105.3
pPP-4	121.8	118.3	114.8	−109.6
oPP-4	123.7	117.3	112.1	−100.8
pPP-5	119.1	114.1	108.8	−101.6
oPP-5	126.1	119.0	113.4	−93.1

Table 6 Melting characteristics of the crystalline phase of PP-NWFs from 2nd DSC heating scan

Sample	T_p/°C	T_{end}/°C	ΔH/mWg^{-1}	Crystalline portion/%
pPP-1	162.5	169.3	100.6	68
oPP-1	169.3	165.0	98.6	67
pPP-2	160.5	168.1	97.9	66
oPP-2	162.9	168.8	86.0	58
pPP-3	163.2	170.2	121.6	82
oPP-3	166.5	170.5	91.7	62
pPP-4	163.9	168.5	98.2	66
oPP-4	164.9	169.4	97.2	66
pPP-5	164.2	170.6	85.0	57
oPP-5	166.0	169.4	83.19	56

Although the oxyfluorinated NWFs were tested several weeks after the oxyfluorination process, long-lived radicals could still be detected on the surfaces of the NWFs as midchain peroxy radicals. This may indicate that the radicals were entrapped in the NWFs during the oxyfluorination process, and slowly diffuse to the surface with time. Also long-lived peroxy radicals will be very useful for inducing graft polymerisation for attachment of poly (*N*-isopropylacryalmide) onto the NWFs.

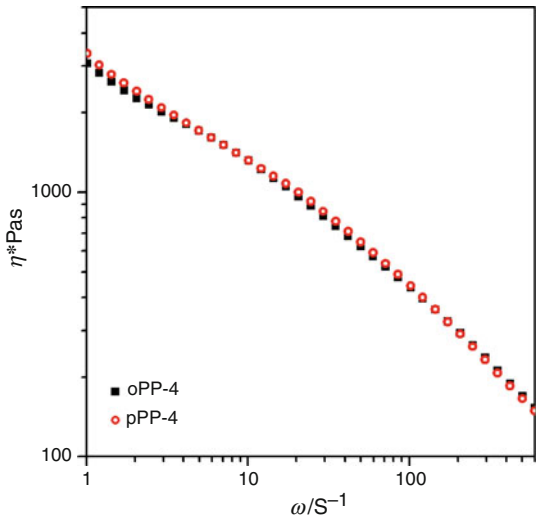

Fig. 12 The change in complex viscosity of virgin and oxyfluorinated sample with frequency at 180 ± 0.2 °C

Further measurements have been carried out at 70 °C, to follow the change in radical concentration with time at the temperature of grafting (Fig. 6). The concentration scale is not calibrated, although the samples are normalised to 1 mg, so that they can be compared. The absolute concentrations are very small, and the signal/noise ratio is ~5, which is rather low. The background noise is rather high. On sample oPP-2 was the easiest to measure the time-dependence of radical concentration at 70 °C. It can be seen that after some increase, the concentration of the radicals does not change. Samples oPP-3 and oPP-5 did not show an increase in radical concentration with time at 70 °C.

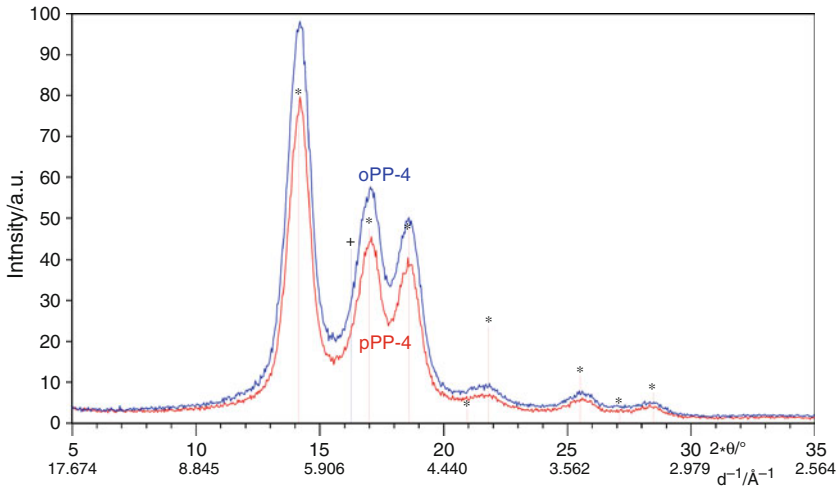

Fig. 11 Typical WAXS diffractogram of NWFs pPP-4 and oPP-4

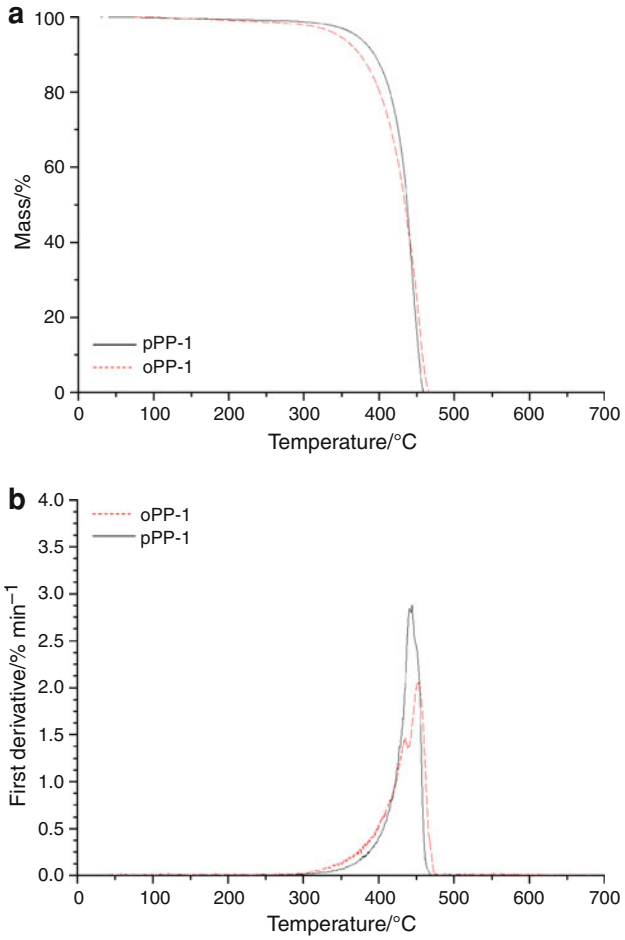

Fig. 13 TG and derivative TG thermograms of virgin and oxyfluorinated PP NWF sample 1 in purging nitrogen

Change of morphology detected by SEM

The micrographs on the virgin and oxyfluorinated PP NWF fibres detected by SEM are represented by Fig. 7. A slight roughening can be detected on the surface of the fibres as a result of surface treatment. This coincides with the findings of other researchers, who have also reported a significant increase in roughening of the surface resulting from the exothermic nature of the oxyfluorination reaction [2, 14]. The possibility of etching of the PP surface during oxyfluorination has also been suggested [2].

From the SEM micrographs the average diameters of the virgin and oxyfluorinated fibres was determined. The results are represented by Fig. 8. As expected the 6.6 dtex linear density fibres had a larger fibre diameter compared to the lower 2.2 dtex linear density fibres. It was also observed that the diameter of the oxyfluorinated fibres is higher, than the untreated ones as a result of surface modification.

Effect of oxyfluorination on the crystallinity of NWF samples

The relaxational and thermal phase transitions of the virgin and oxyfluorinated PP NWF samples were determined by DSC measurement. The T_g was determined with the Perkin Elmer Pyris sotware. T_g was given as half Cp extrapolated. The glass transition of the samples could not always be detected by DSC analysis because of the small enthalpy change (Table 4). It has been found that the T_g was between −5.8 and +5.4 °C. It is difficult to draw any conclusion on the effect of oxyfluorination on the glass transition temperature of PP NWFs from DSC measurement.

Crystallisation and melting of the crystalline phase were investigated in the temperature range of 100–200 °C. During the first heating step of all the samples the melting of the crystalline phase was detected by the appearance of split enthalpy peaks for all the samples as demonstrated by Fig. 9. The reason of the noisy pattern is the contraction of highly extended material therefore its contact to the pan

Table 7 Onset and end temperatures of thermal decomposition of oxyfluorinated PP NWF samples (oPPs) and the corresponding masses of oxyfluorinated (oPPs) and untreated, virgin PP (pPPs) determined from the TG curves

Sample		pPP			oPP		
		Temperatue/ °C	Mass/ %	oPP mass/ %	Temperatue/ °C	Mass/ %	pPP mass/ %
1	Onset	308	98.9	97.7	300	98.1	98.7
	End	460	0.0	9.5	464	0.0	0.0
2	Onset	335	99.2	95.6	312	97.4	99.1
	End	472	0.0	1.7	474	1.0	0.0
3	Onset	329	97.5	95.5	295	97.6	97.5
	End	472	0.0	0.0	455	0.0	27.6
4	Onset	318	99.3	96.6	317	97.0	98.9
	End	468	0.0	2.8	475	0.0	0.0
5	Onset	328	97.9	96.8	298	98.0	98.0
	End	66	0.0	2.0	466	0.3	0.8

Table 8 Characteristic data of thermal decomposition of oxyfluorinated PP NWF samples (oPPs) and the corresponding untreated, virgin PP (pPPs) determined from the first derivative of the TG curves

		pPP			oPP		
		Temperature/°C	Mass/%	oPP mass/%	Temperature/°C	Mass/%	pPP mass/%
1	Onset 1	294	98.8	98.0	283	98.2	98.9
	Shoulder	–	–	–	436	48.2	54.2
	Onset 2	–	–	–	432	52.9	60.5
	Peak	441	39.9	40.3	453	19.7	9.7
	End	468	0.0	0.0	474	0.0	0.0
2	Onset1	338	98.6	95.5	294	97.4	99.3
	Shoulder	–	–	–	425	58.7	61.0
	Onset 2	–	–	–	433	50.1	54.7
	Peak	476	28.5	25.8	452	22.2	15.3
	End	445	0.0	1.2	476	1.2	0.0
3	Onset 1	316	97.3	96.5	300	97.1	97.5
	Shoulder	–	–	–	423	49.3	75.8
	Onset 2	–	–	–	417	56.4	79.7
	Peak	452	33.4	3.0	442	19.9	53.4
	End	481	0.0	0.0	463	0.0	10.2
4	Onset 1	299	99.2	97.1	281	97.4	99.3
	Shoulder	–	–	–	456	50.3	69.2
	Onset 2	–	–	–	432	52.0	72.6
	Peak	448	36.0	32.9	434	51.1	15.2
	End	479	0.0	0.0	480	0.0	0.0
5	Onset 1	347	97.4	95.4	305	97.6	97.9
	Shoulder	–	–	–	431	51.0	72.8
	Onset 2	–	–	–	417	68.1	85.7
	Peak	431	35.1	27.5	453	19.5	23.2
	End	476	0.0	0.2	474	0.2	0.0

changes. However, the first heating run could give real information about the changes in the properties. More appropriate experimental technique would be necessary to get real data from the first heating run, such as temperature-modulated DSC [25]. Thermal prehistory was eliminated by the first heating step, and crystallisation and melting were investigated during the cooling and second heating step of DSC measurements. After the melting of the fibres, the system is not homogeneous, the fluorinated part can be regarded as separated from the main phase. Purpose of this measurement was the calculation of crystalline portion before and after oxyfluorination. The results are represented on NWF sample 2 by Fig. 10, and the evaluation of the data on crystallisation and melting are summarised in Tables 5 and 6.

The oxyfluorinated NWFs crystallise at somewhat higher temperatures than the untreated NWFs (Table 5). The endotherm peak on the DSC curve of the second heating represents the melting of the crystalline phase of the PP samples (Table 6). The asymmetry of the peaks may be due to the formation of more stable crystalline forms during the heating procedure. This phenomenon had been reported previously for isotactic PP [26, 27]. Considering the melting characteristics of the crystalline phase of NWF samples from Table 6, the melting peak temperature of the oxyfluorinated PP samples is somewhat higher than that of the untreated ones. There is no significant difference in the end temperature of melting of the untreated and functionalised PP samples. The enthalpy of melting is somewhat lower for the oxyfluorinated PP non-wovens compared with the virgin, untreated ones, referring to slight decrease in the ratio of the crystalline phase in relation to the amorphous after oxyfluorination (Table 6). In case of NWF sample 3, there is a significant (20%) decrease in the crystalline phase after oxyfluorination, and the elucidation of this needs further investigation. The crystalline portion was calculated according to Monasse and Haudin [28].

The effect of oxyfluorination on crystallinity has also been investigated by WAXS. The WAXS diffractograms for NWF sample 4 are shown by Fig. 11, from which the

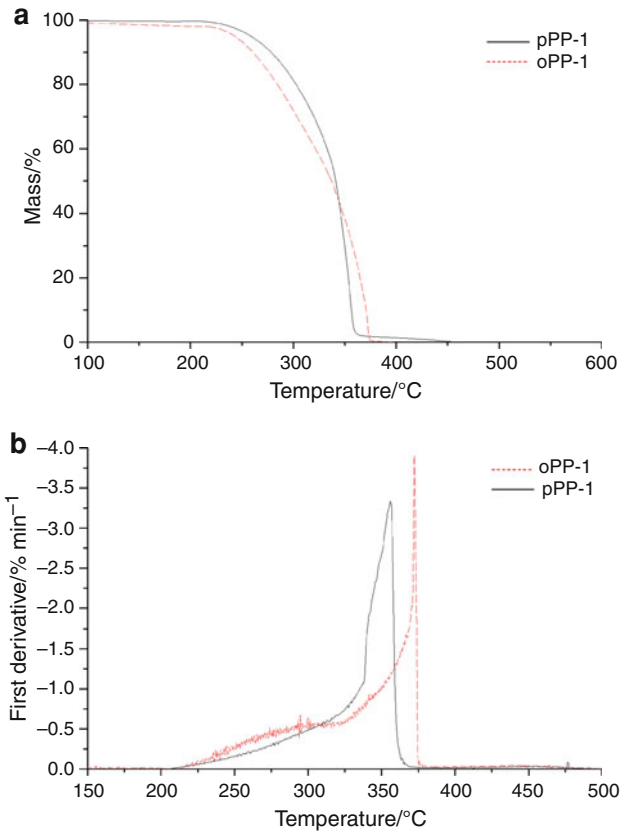

Fig. 14 TG and derivative TG thermograms of virgin and oxyfluorinated PP NWF sample 1 in purging oxygen

differences of the absolute intensities can be read. Owing to sample geometry neither the absolute nor the relative intensities can be compared. The diffraction peaks however, for the treated and untreated NWFs were the same indicating that the oxyfluorination treatment had no effect on the crystalline structure or crystalline phases in PP. The ratio of amorphous and crystalline phases has been calculated by profile fitting. The fitting of the amorphous quantity is not better than ±5%. Differences may arise from the deviations of sample thickness, sample size etc. WAXS measurements support that oxyfluorination does not have significant effect on the crystallinity and phase composition of PP NWFs.

Based on the results of both of DSC and XRD measurements, we can state that oxyfluorination had no significant effect on the crystallinity and crystalline/amorphous phase compositions of PP NWF samples.

Effect of oxyfluorination on the molecular mass of PP NWF samples

The effect of oxyfluorination on the change of molecular mass of PP NWFs was determined using dynamic rheometry. The results are shown by Fig. 12, indicating that the melt viscosity of PP is unaffected by the oxyfluorination treatment, implying that the molecular mass of the PP NWFs does not significantly change after oxyfluorination.

Thermal behaviour detected by TG

The effects of oxyfluorination on the thermal and thermo-oxidative stabilities and decompositions of PP NWFs were studied by TG analysis. The curves in purging nitrogen refer to the thermal stability of the samples and are represented on NWF sample 1 by Fig. 13. There are two important differences in the thermal decompositions of virgin and oxyfluorinated PP samples. The onset of thermal decomposition of the oxyfluorinated PP samples is lower than that of the untreated ones, and the mass loss is higher than that in case of pure PP because of higher moisture absorption and partial decomposition of functional groups

Table 9 Onset and end temperatures of thermo-oxidative decomposition of oxyfluorinated PP NWF samples (oPPs) and the corresponding masses of oxyfluorinated (oPPs) and untreated, virgin PP (pPPs) determined from the TG curves

Sample		pPP			oPP		
		Temperatue/ °C	Mass/ %	oPP mass/%	Temperatue/ °C	Mass/ %	pPP mass/%
1	Onset	227	99.5	97.5227	97.8	99.0	
	End	361	1.9	24.9	374	0.5	1.6
2	Onset	223	99.9	98.5	224	98.8	99.5
	End	356	3.7	34.4	369	5.0	3.4
3	Onset	226	99.8	0.0	240	99.6	97.4
	End	369	2.6	35.4	388	4.6	2.1
4	Onset	218	99.8	99.2	230	99.0	98.3
	End	362	3.3	32.6	382	2.6	3.0
5	Onset	233	99.9	98.2	232	98.7	99.2
	End	360	5.5	24.7	372	4.1	5.3

Table 10 Characteristic data of thermo-oxidative decomposition of oxyfluorinated PP NWF samples (oPPs) and the corresponding untreated, virgin PP (pPPs) determined from the 1st derivative of the TG curves

Sample		pPP			oPP		
		Temperatue/ °C	Mass/ %	oPP mass/%	Temperatue/ °C	Mass/ %	pPP mass/%
1	Onset 1	211	99.7	98.1	217	98.1	99.5
	Shoulder-	–	–	304	69.6	79.2	
	Onset 2	–	–	–	324	58.5	67.1
	Peak	356	11.7	31.6	372	5.0	1.8
	End	367	1.9	16.9	375	0.5	1.7
2	Onset 1	210	100.0	99.0	208	99.0	100.0
	Shoulder-	–	–	277	84.2	87.5	
	Onset 2	–	–	–	308	71.2	71.0
	Peak	345	20.6	49.4	366	15.6	3.5
	End	360	3.8	29.0	370	5.1	3.4
3	Onset 1	208	99.9	99.8	232	99.8	98.6
	Shoulder-	–	–	296	79.3	79.5	
	Onset 2	–	–	–	325	65.8	59.4
	Peak	354	18.1	49.0	385	11.4	2.3
	End	370	2.7	33.1	389	4.9	2.2
4	Onset 1	208	99.9	99.2	219	99.2	99.5
	Shoulder	–	–	–	–	–	–
	Onset 2	–	–	–	–	–	–
	Peak	357	12.2	38.7	379	8.5	2.9
	End	365	3.4	30.2	382	2.9	2.9
5	Onset 1	229	99.4	98.5	227	98.7	99.6
	Shoulder	299	64.0	73.3	–	–	–
	Onset 2	321	43.4	61.0	–	–	–
	Peak	343	19.1	44.7	370	7.0	5.3
	End	358	6.0	27.0	373	5.2	4.2

on the surface. Owing to the presence of functional groups on the surface of oxyfluorinated samples, the mechanism of thermal decomposition is also different from that of the virgin PP non-woven ones. As the derivative curves show, oxyfluorinated NWFs decompose in two steps compared to the pure PP NWFs which decompose in one step. The evaluation of the curves and derivative curves detected in purging nitrogen are summarised in Tables 7 and 8.

The TG and derivative TG curves of the untreated and oxyfluorinated NWF sample 1 in purging oxygen are shown in Fig. 14. The evaluations of the corresponding TG and derivative TG curves of all the NWFs are summarised in Tables 9 and 10.

The thermo-oxidative decompositions of the untreated and oxyfluorinated PP NWF samples are very similar. The onset of thermo-oxidative decomposition is almost the same, namely in the range of 218–240 °C. In the case of samples 3 and 4, the thermo-oxidative decompositions of the oxyfluorinated NWFs take place at higher temperature, than for the untreated PP ones. Thermo-oxidative decomposition takes place in two steps for each sample, the first steps are roughly in the same temperature range beginning with the onset and ending in the vicinity of 300 °C. The second step, however, is at much higher range of temperature for the oxyfluorinated samples.

Summary

Surface functionalisation of PP NWF samples of different morphologies and pore sizes has been carried out by oxyfluorination. The functionalised surfaces have been characterised for functional groups by ATR-FTIR spectroscopy, XPS analysis and ESR-spectroscopy. ATR-FTIR and XPS techniques revealed the presence of –CF, $–CF_2$, –CHF and –C(O)F groups. The formed –C(O)F groups mostly get hydrolysed to –COOH groups. The C=O stretching vibration of alpha-haloester, and the C=C

stretching of the formed –CF=C(OH)– groups could also be detected. Long-lived radicals could be detected on the functionalised surfaces, as middle-chain peroxy radicals by ESR-spectroscopy. Three samples (oPP-1, oPP-2 and oPP-4 showed a slight increase in radical concentration with time at 70 °C (temperature of grafting). SEM micrographs revealed slight roughening of the oxyfluorinated surfaces. Oxyfluorination had no significant effect on the crystalline structure and crystalline/amorphous phase composition of the PP NWF samples supported by DSC and XRD measurements. Oxyfluorinaton did not significantly effect the molecular mass of PP as confirmed by dynamic rheometry. Surface modification, however, significantly affected the thermal decomposition and mechanism of PP NWFs. Thermo-oxidative decomposition of untreated and oxyfluorinated PP NWFs were very similar. Morphology and pore size of PP NWF samples had no significant effect on surface functionalisation.

Acknowledgements The authors thank the Hungarian Science and Technology Foundation ZA-9/2006, the National Science Foundation (South Africa), and the CSIR (South Africa) for financial support The authors are also grateful to Pelchem Pty Ltd (in South Africa) for the oxyfluroination treatments on all the NWFs. The authors thank also János Kovács for dynamic rheological assistance, and József Hári for SEM measurements.

References

1. du Toit FJ, Sanderson RD, Engelbrecht WJ, Wagener JB. The effect of surface fluorination on the wettability of high density polyethylene. J Fluor Chem. 1995;74(1):43–8.
2. du Toit FJ, Sanderson RD. Surface fluorination of polypropylene: 1. characterisation of surface properties. J Fluor Chem. 1999; 98(2):107–14.
3. du Toit FJ, Sanderson RD. Surface fluorination of polypropylene: 2. adhesion properties. J Fluor Chem. 1999;98(2):115–9.
4. Mohr JM, Paul DR, Tam Y, Mlsna TE, Lagow RJ. Surface fluorination of composite membranes. Part II. Characterization of the fluorinated layer. J Membr Sci. 1991;55(1–2):149–71.
5. Brass I, Brewis DM, Sutherland I, Wiktorowicz R. The effect of fluorination on adhesion to polyethylene. Int J Adhes Adhes. 1991;11(3):150–3.
6. Park SJ, Song SY, Shin JS, Rhee JM. Effect of surface oxyfluorination on the dyeability of polyethylene film. J Colloid Interface Sci. 2005;283(1):190–5.
7. Sanderson R, du Toit F, Carstens P, Wagener J. Fluorination rates of polyolefins as a function of structure and gas atmosphere. J Therm Anal Calorim. 1994;41(2):563–81.
8. Lagow RJ, Margrave JL. Direct fluorination: a "new" approach to fluorine chemistry. progress in inorganic chemistry. Hoboken: John Wiley & Sons, Inc; 2007.
9. Shimada J, Hoshino M. Surface fluorination of transparent polymer film. J Appl Polym Sci. 1975;19(5):1439–48.
10. Hayes LJ. Surface energy of fluorinated surfaces. J Fluor Chem. 1976;8(1):69–88.
11. Leroux JD, Paul DR, Arendt MF, Yuan Y, Cabasso I. Surface fluorination of poly(phenylene oxide) composite membranes. 2. Characterization of the fluorinated layer. J Membr Sci. 1994; 90(1–2):37–53.
12. Volkmann T, Widdecke H. Oxifluorination of polyethylene. Kunstst Ger Plast. 1989;79(8):743–4.
13. Jeong E, Bae T-S, Yun S-M, Woo S-W, Lee Y-S. Surface characteristics of low-density polyethylene films modified by oxyfluorination-assisted graft polymerization. Colloids Surf A. 2011;373(1–3):36–41.
14. du Toit FJ. Surface modification of polymers using elemental flourine. Ph.D. Thesis, University of Stellenbosch; 1995.
15. Kharitonov AP. Practical applications of the direct fluorination of polymers. J Fluor Chem. 2000;103(2):123–7.
16. Kharitonov AP, Taege R, Ferrier G, Teplyakov VV, Syrtsova DA, Koops G-H. Direct fluorination—useful tool to enhance commercial properties of polymer articles. J Fluor Chem. 2005;126(2):251–63.
17. Tressaud A, Durand E, Labrugère C, Kharitonov AP, Kharitonova LN. Modification of surface properties of carbon-based and polymeric materials through fluorination routes: from fundamental research to industrial applications. J Fluor Chem. 2007; 128(4):378–91.
18. Kharitonov AP, Kharitonova LN. Surface modification of polymers by direct fluorination: a convenient approach to improve commercial properties of polymeric articles. Pure Appl Chem. 2009;81(3):451–71.
19. Boguslavsky L. High efficiency particulate air (HEPA) Filters from polyester and polypropylene -Nonwovens,. International Conference FILTREX 2010; October; Cologne, Germany 2010.
20. Socrates G. Infrared and Raman characteristic group frequencies : tables and charts. 3 ed. ed. Wiley: Chichester; 2001.
21. Kharitonov AP. Direct fluorination of polymers—from fundamental research to industrial applications. Prog Org Coat. 2008;61(2–4):192–204.
22. Mihaly J, Sterkel S, Ortner HM, Kocsis L, Hajba L, Furdyga E, et al. FTIR and FT-Raman spectroscopic study on polymer based high pressure digestion vessels. Croatica Chemica Acta. 2006; 79:497–501.
23. Beamson G, Briggs D. High resolution XPS of organic polymers. The scienta ESCA300 database. Chichester: Wiley; 1992.
24. Schlick S, Mcgarvey BR. Motion of midchain peroxy-radicals in poly(tetrafluoroethylene). J Phys Chem. 1983;87(2):352–3.
25. Genovese A, Shanks R. Crystallization and melting of isotactic polypropylene in response to temperature modulation. J Therm Anal Calorim. 2004;75(1):233–48.
26. Horvath Z, Sajo IE, Stoll K, Menyhard A, Varga J. The effect of molecular mass on the polymorphism and crystalline structure of isotactic polypropylene. eXPRESS Polym Lett. 2010;4(2): 101–14.
27. Nurul Huda M, Dragaun H, Bauer S, Muschik H, Skalicky P. A study of the crystallinity index of polypropylene fibres. Colloid Polym Sci. 1985;263(9):730–7.
28. Monasse B, Haudin JM. Growth transition and morphology change in polypropylene. Colloid Polym Sci. 1985;263(10): 822–31.